Inorganica Chimica Acta 423 (2014) 123–132

Contents lists available at ScienceDirect

Inorganica Chimica Acta

journal homepage: www.elsevier.com/locate/ica

A dynamic metal–organic supramolecular host based on weak π-stacking interactions incorporating 2D water-chloride-methanolic supramolecular sheet

Rajat Saha [a], Somen Goswami [a], Susobhan Biswas [a], Ian M. Steele [c], Kamalendu Dey [b,*], Atish Dipankar Jana [d,*], Sanjay Kumar [a,*]

[a] Department of Physics, Jadavpur University, Jadavpur, Kolkata 700032, India
[b] Department of Chemistry, University of Kalyani, Kalyani 741235, West Bengal, India
[c] Department of the Geophysical Sciences, The University of Chicago, Chicago, USA
[d] Department of Physics, Behala College, Parnasree, Kolkata 700060, India

ARTICLE INFO

Article history:
Received 8 June 2014
Received in revised form 20 July 2014
Accepted 27 July 2014
Available online 12 August 2014

Keywords:
Cationic metal–organic complex
π···π interaction
2D water-chloride-methanolic supramolecular sheet
Dynamic host
Photoluminescence

ABSTRACT

Herein, we report the formation of a unique water-chloride-methanol 2D supramolecular network within the hydrophobic interlayer cavities of a novel flexible metal–organic supramolecular host (MOSH) framework formed by π-induced self-assembly of the monomeric metal–organic complex $[Pr(1,10\text{-phen})_2(H_2O)_5]Cl_3(H_2O)(CH_3OH)$ (1,10-phen = 1,10-phenanthroline) (**complex 1**). Single crystal X-ray diffraction (SC-XRD), powder X-ray diffraction (PXRD) and spectroscopic techniques are used to characterize the complex. The structural analysis reveals that in this MOSH the discrete metal–organic moieties are connected by π···π interactions to form 2D metal–organic supramolecular sheet structures. The guest water and methanol molecules together with counter chloride anions stabilize in the MOSH framework through hydrogen bonding interactions between the 2D metal–organic supramolecular layers. The hydrogen bonding interactions among the coordinated water and guest species form a unique 2D supramolecular water-chloride-methanol sheet structure. Upon removal of guest water and methanol molecules by heat treatment the supramolecular framework gets shrunk but retains the crystallinity while upon re-absorption of water molecules it undergoes structural change with expansion of effective guest accessible void space. The flexibility of the supramolecular framework and the mechanism of thermally induced phase transformation in the MOSH are examined by PXRD study. The photoluminescence property of the **complex 1** and the crystalline complex obtained after rehydration has been thoroughly investigated. The theoretical analysis has been performed to resolve the issue of stability of the 2D supramolecular water-chloride-methanol sheet in the MOSH framework and it has been found that for **complex 1** the stabilization energy of the $[(H_2O)_6\text{-}(CH_3OH)\text{-}Cl_3]_n^{3-}$ is 1949.427Kcal mol^{-1}.

© 2014 Elsevier B.V. All rights reserved.

1. Introduction

The self-assembly of discrete molecular units via covalent or non-covalent interactions, such as, hydrogen-bonding, π-stacking interactions, etc. is a popular approach for design and synthesis of new compounds having wide range of application potential [1–6]. During self assembly the discrete metal–organic moieties connect themselves through cooperative non-covalent interactions and this leads to formation of metal–organic supramolecular host (MOSH) [7–12]. The guest molecules get stability in the MOSHs through supramolecular interactions. The MOSHs can very efficiently release and absorb guest molecules in a controlled manner [13–14]. Depending on the design strategy, the MOSHs are classified in two broad categories, viz., charged MOSH and uncharged MOSH. The uncharged MOSHs are capable of accommodating neutral guest species like simple water clusters [15–19], whereas the cationic MOSHs can easily accommodate anionic guest species like chloride-hydrates [20–24]. Since the ion transportation is a very important phenomenon in various chemical and biological processes in the living systems [25–29], several novel strategies have been adopted for recognition and transportation of ions in the self-assembled complexes [30–31]. The self-assembly is one of the unique approaches for construction of ion channels in cationic

* Corresponding authors. Tel.: +91 9831115427; fax: +91 33 2413 8917 (S. Kumar).
E-mail addresses: kdey_chem.@rediffmail.com (K. Dey), atishdipankarjana@yahoo.in (A.D. Jana), kumars@phys.jdvu.ac.in (S. Kumar).

http://dx.doi.org/10.1016/j.ica.2014.07.077
0020-1693/© 2014 Elsevier B.V. All rights reserved.

MOFs. The cationic metal–organic complex formation can be realized without using any anionic donor ligands.

Studies on water clusters in metal–organic host complexes have attracted a great deal of attention during recent times [32–36]. On the other hand, hybrid clusters of water and other small organic molecules or ions formed by hydrogen bonding interaction have drawn relatively less attention. In particular, there are very few reports on experimental identification and analysis of discrete water-chloride clusters (the hydrogen-bonded assemblies of water on crystallization and chloride counter ions in crystalline materials) [19–24]. The hydration phenomenon of chloride ion has canonical importance in the field of biochemistry [37] and supramolecular chemistry. Moreover, drug molecules are generally organic molecules and they dissolve in organic solvents like methanol, ethanol, etc. For efficient delivery of the anionic drug molecules a better understanding of the mode of interaction of the anions with organic solvents and water is a prerequisite. More than 70% of enzymes, substrates and cofactors are anions. Thus, more theoretical and experimental investigations on hybrid water-chloride clusters with other organic molecules are very essential taste.

In this context, we have reported previously the formation of a 2D water sheet, a helical-water chain and water-chloride tape in chiral supramolecular complexes and supramolecular hosts [38,39]. As a continuing effort, in this report, we have shown that a water-chloride-methanol 2D supramolecular network can be created within the hydrophobic interlayer cavities of a dynamic MOSH. A simple strategy that can be adopted for possible isolation of a hybrid water-chloride system is to use a neutral ligand in synthesizing Pr(III)-based cationic complexes. In this effort, we have successfully synthesized a metal–organic complex [Pr(1,10-phen)$_2$(H_2O)$_5$] Cl_3(H_2O)(CH_3OH), which includes water, chloride and methanol as guest molecules using 1,10-phenanthroline ligand. It is expected that the chelating nature of 1,10-phenanthroline along with its inherent π-stacking capability would integrate the discrete metal moieties at least in one direction. The X-ray crystal structure analysis has revealed that the complex assembles into a 2D supramolecular architecture through π···π interactions. The complex behaves like a dynamic metal–organic supramolecular host (MOSH). Three chloride ions, one guest water molecule and one guest methanol molecule along with five coordinated water molecules form unique water-chloride-methanol hybrid 2D hydrogen bonded network and is stabilized within the hydrophobic interlayer cavities. The most important property of the present MOSH is its breathing nature – when the host is heated up it expels the guest molecules and during cooling the species absorbs the water molecules from the atmosphere. The dynamic breathing metal–organic frameworks (MOFs) are easy to design but a dynamic supramolecular host like the present one is rarely observed as it requires involvement of weak forces. The present work shows how weak π···π stacking forces can be employed in designing host–guest frameworks and may work as effective example in designing new dynamic MOSHs.

2. Experimental

2.1. General

The ingredients praseodymium (III) chloride, hepta-hydrate and 1,10-phenanthroline were purchased from Merck Chemical Company and all other chemicals used were AR grade. The elemental analysis (C, H and N) was carried out using a Perkin-Elmer 240C elemental analyzer. The IR spectrum was recorded between 400 and 4000 cm^{-1} using a Nicolet Impact 410 spectrometer employing the KBr pellet method. The thermal analysis was carried out using a Mettler Toledo TGA-DTA 85 thermal analyzer under a flow of N_2 (30 ml min^{-1}). The sample was heated at a rate of 10 °C min^{-1} with inert alumina as a reference. The photoluminescence spectra were collected on a Shimadzu RF-5301PC Spectrophotometer. The Powder X-ray diffraction (PXRD) patterns were recorded by using Cu-K_α radiation (Bruker D8; 40 kV, 40 mA).

2.2. Synthesis of **complex 1** {[Pr(1,10-phen)$_2$(H_2O)$_5$]Cl_3(H_2O)(CH_3OH)}

5 ml aqueous solution of $PrCl_3 \cdot 7H_2O$ (0.93 g, 0.0025 mol) was added drop-wise to a solution of 1,10-phenanthroline (0.90 g, 0.005 mol) in MeOH (5 ml). The resulting solution was then filtered off and was kept in open air. After 10 days, the light greenish yellow colored single crystals suitable for single crystal X-ray (SCXRD) study appeared and they were collected by filtration. Yield: 1.40 g (75% based on Pr). *Anal.* Calc. for $C_{25}H_{32}PrN_4O_7Cl_3$: C, 40.15; H, 4.31; N, 7.49. Found: C, 40.02; H, 4.39; N, 7.36%. IR (KBr, cm^{-1}): 3332br, 2298vw, 1627s, 1593s, 1574s, 1518s, 1421 m, 1343s, 1299m, 1102m, 1091w, 863m, 846s, 772s, 722w, 635w. λ_{max} (in MeOH) 260 nm, 324 nm (shoulder).

2.3. Crystallographic data collection and refinement

The suitable single crystal of the **complex** was mounted on a Bruker SMART diffractometer equipped with a graphite monochromator and Mo Kα (λ = 0.71073 Å) radiation and the data was collected at room temperature. The structure was solved by Patterson method using the SHELXS97 program. The hydrogen atoms were placed in idealized positions and their displacement parameters were fixed to be 1.2 times larger than those of the attached non-hydrogen atoms. The position of non-hydrogen atoms were refined with independent anisotropic displacement parameters. The subsequent difference Fourier synthesis and least-square refinement revealed the positions of the non-hydrogen atoms. The successful convergence was indicated by the maximum shift/error of 0.001 for the last cycle of the least square refinement. All calculations were carried out using SHELXS 97 [40], SHELXL 97 [41], PLATON 99 [42], ORTEP-32 [43] and WinGX system Ver-1.64 [44]. The data collection, structure refinement parameters and crystallographic data of **complex 1** are provided in Table 1.

3. Results and discussion

3.1. Crystal structure of **complex 1** {[Pr(1,10-phen)$_2$(H_2O)$_5$]Cl_3(H_2O)(CH_3OH)}

The analysis of SCXRD data have revealed that **complex 1** is a neutral mononuclear compound in which the Pr^{3+} ion is coordinated to two different 1,10-phen ligands and five water molecules as shown in Fig. 1. Each asymmetric unit contains one metal–organic moiety, three chloride anions, one guest methanol molecule and one guest water molecule. In the present case Pr(III) shows nine coordination mode. The four nitrogen atoms (N1, N2, N3 and N4) of two different 1,10-phen ligands and five water molecules (O1W, O2W, O3W, O4W and O5W) fulfill the nine coordination of Pr(III) through formation of a paddle-wheel shaped molecular structure. Some selected coordination bond lengths and bond angles are listed in Table 2 and 3, respectively. The two 1,10-phen moieties are nearly at the *trans* position to each other. The Pr–N bond lengths lie between 2.662(2) and 2.723(2) Å which are well within the range of other reported Pr(III)-phen complexes [45–48]. It is well known that the lanthanide ions have high affinity for hard donor atoms and ligands with oxygen or hybrid oxygen–nitrogen atoms [49]. The Pr–O_{water} distances are in the range between 2.448(2) and 2.487(2) Å (average 2.477 Å), which are comparable with those observed in other Pr^{3+} ion complexes with

Table 1
Crystallographic data and refinement parameters of **complex 1**.

Crystal data	
Formula	$C_{24}H_{26}N_4O_5Pr$, CH_4O, H_2O, 3Cl
Formula weight	747.81
Crystal system	triclinic
Space group	$P\bar{1}$ (No. 2)
a [Å]	8.872(3)
b [Å]	9.192(3)
c [Å]	18.920(6)
α [°]	88.790(5)
β [°]	84.689(5)
γ [°]	69.159(5)
V [Å^3]	1435.7(8)
Z	2
D_{calc} [g cm^{-3}]	1.730
μ (Mo Kα) [mm^{-1}]	2.027
F(000)	752
Data collection	
Temperature (K)	100
Radiation [Å]	Mo Kα 0.71073
Theta min–max [°]	1.1, 28.4
Dataset	−11: 11; −12: 12; −25: 24
Total	16947
Unique data	6698
R_{int}	0.015
Observed data [$I > 2\sigma(I)$]	6510
Refinement	
Nref, Npar	6698; 361
R	0.0276
wR_2	0.0717
S	1.06
Maximum and average shift/error	0.00, 0.00
Minimum and maximum residual density [e Å^{-3}]	−0.91, 1.51

Table 2
Selected bond lengths (Å) of **complex 1**.

Bonds	Bond distance	Bonds	Bond distance
Pr1–O1W	2.4826(19)	Pr1–O2W	2.484(2)
Pr1–O3W	2.487(2)	Pr1–O4W	2.448(2)
Pr1–O5W	2.481(3)	Pr1–N1	2.709(2)
Pr1–N2	2.662(2)	Pr1–N3	2.723(2)
Pr1–N4	2.677(2)		

analogous ligands [48]. It is noteworthy that the monomeric units are further connected by supramolecular hydrogen bonding and π···interactions with the guest molecules to form a 3D supramolecular structure.

3.2. Supramolecular structure

In the present system, the monomeric metal–organic units are connected by supramolecular π-interactions to from 2D supramolecular sheets and between two 2D supramolecular sheets one guest methanol molecule, one guest water molecule and three charge neutralized chloride ions are accumulated by self-assembly. The pyridyl ring [Cg1] of the 1,10-phen ligand in one metal–organic unit bridges the phenyl ring [Cg5] of a symmetry [2 − x, −y, 1 − z] related metal–organic unit. Again, the pyridyl ring [Cg4] of the same 1,10-phen unit interacts with another phenyl ring [Cg6] of the same symmetry [2 − x, −y, −z] related unit. In this way, the monomeric units are connected to form 1D supramolecular chains along the crystallographic c-axis as shown in Fig. 2. These 1D supramolecular chains are further connected by π···π interactions to form 2D supramolecular sheets within the ac-plane, (Fig. 3). The pyridyl ring [Cg2] of one 1,10-phen unit connects the self-complementary pyridyl ring [Cg2] of a symmetry related [1 − x, −y, 1 − z] nearby unit. All the π···π interaction parameters are summarized in Table 4. The 2D supramolecular sheets are packed along b-axis to form metal–organic supramolecular hosts (Fig. 4) bearing hydrophobic pockets lined up by the 1,10-phen ligands. These hydrophobic pockets are filled up by one water molecule, one methanol molecule and three counter chloride ions. All these guest molecules interact with the metal–organic moieties through hydrogen bonding interactions. Among the guest species, only Cl1 is connected with the framework by hydrogen bonding interactions as shown in Figure S1. Two chloride ions, one water molecule and one methanol molecule form a [$Cl_2(H_2O)$(MeOH)] cluster by hydrogen bonding interactions as shown in Figure S2.

The hydrogen bonding interactions between the coordinated water molecules and the guest species have formed a 2D supramolecular network in the crystallographic ab-plane (Figs. 5 & S3). Cl1 is bound to H2W2 of O2W water molecule and the other hydrogen atom H1W2 is connected with methanolic oxygen atom O1. O1 is also connected with H2W1 of O1W water molecule. Methanolic hydrogen atom H1O1 is attached with Cl3. The other hydrogen atom H1W1 is bound to atom Cl2 and Cl2 binds the H2W5 of O5W water molecule. Other hydrogen atom H1W5 is bound to Cl1. This Cl1 is also connected with the H1W4 of O4W water molecule. Second hydrogen atom H2W4 of O4W binds the Cl3 atom which is consequently bound to H1W6 of O6W. The other hydrogen atom H2W6 of O6W has formed bond with Cl2 while Cl2 is bound to H2W3 of O3W water molecule and H1W3 of O3W is connected with Cl1, which is bound to H2W2. All these together build

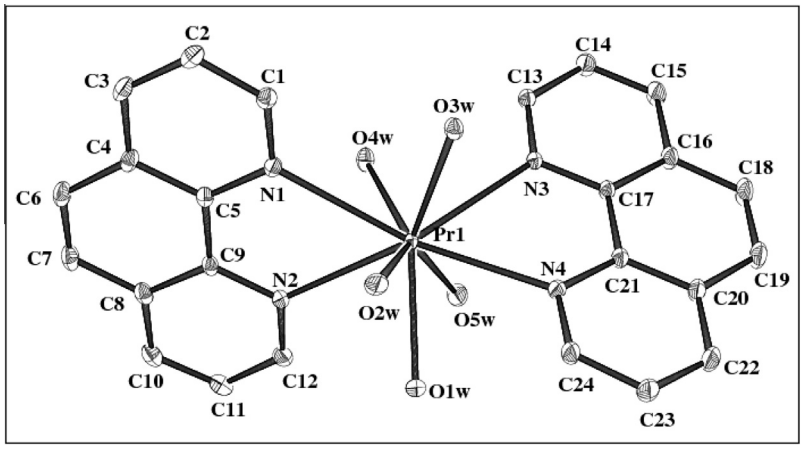

Fig. 1. The ORTEP diagram of **complex 1**.

Table 3
Selected bond angles (°) of **complex 1**.

O1W–Pr1–O2W	70.13(8)	O5W–Pr1–N3	69.76(6)
O1W–Pr1–O3W	132.85(7)	O5W–Pr1–N4	78.94(6)
O1W–Pr1–O4W	131.25(7)	N1–Pr1–N2	61.66(6)
O1W–Pr1–O5W	70.69(8)	N1–Pr1–N3	121.07(5)
O1W–Pr1–N1	117.99(6)	N1–Pr1–N4	148.66(6)
O1W–Pr1–N2	71.28(6)	N2–Pr1–N3	139.58(6)
O1W–Pr1–N3	120.93(6)	N2–Pr1–N4	139.99(5)
O1W–Pr1–N4	69.50(6)	N3–Pr1–N4	61.26(5)
O2W–Pr1–O3W	72.48(6)	O2W–Pr1–O4W	140.55(6)
O2W–Pr1–O5W	140.40(6)	O2W–Pr1–N1	73.26(6)
O2W–Pr1–N2	91.74(6)	O2W–Pr1–N3	128.55(6)
O2W–Pr1–N4	82.37(6)	O3W–Pr1–O4W	95.90(6)
O3W–Pr1–O5W	135.36(6)	O3W–Pr1–N1	76.02(6)
O3W–Pr1–N2	137.58(6)	O3W–Pr1–N3	65.66(6)
O3W–Pr1–N4	78.07(6)	O4W–Pr1–O5W	73.53(6)
O4W–Pr1–N1	67.32(6)	O4W–Pr1–N2	71.39(6)
O4W–Pr1–N3	73.85(6)	O4W–Pr1–N4	133.18(6)
O5W–Pr1–N1	132.31(6)	O5W–Pr1–N2	81.04(6)

up a supramolecular 2D sheet of $\{(H_2O)_6\text{-}(CH_3OH)\text{-}Cl_3\}_n$. The hydrogen bonding association of the guest with the host leads to the formation of a 3D supramolecular assembly of the host–guest framework (Figure S4). All the hydrogen bonding interactions are summarized in Table 5.

3.3. Thermal analysis

We have studied the thermal stability of the complex (Fig. 6). The thermogravimetric analysis shows a weight loss of 12.43% (calculated 13.91%) in the temperature range between 40 and 117 °C which corresponds to the loss of one lattice water molecule, one methanol molecule and three coordinated water molecules. A further weight loss of 3.96% occurs between 117 and 257 °C consistent with the loss of two coordinated water molecules (calculated 4.82%). The observed weight losses are a little bit lower than the theoretical values. The slight discrepancy is due to weight loss occurring even at lower than 40 °C, illustrating the dynamic nature of the water molecules in the solid state.

3.4. Study on dynamic nature of the host–guest binding-removal and reintroduction of guests

The rigid metal–organic coordination polymers have attracted considerable interest because of their potential applications in catalysis, adsorption and ion exchange [50–52]. However, the flexible metal–organic frameworks are more efficient for these applications [53–56], as flexible frameworks are very sensitive to the presence of guests and undergo structural changes depending upon the number and nature of the guest molecules [57–60]. The thermal study of **complex 1** has revealed that within 117 °C one guest water molecule, one methanol molecule and three coordinated water molecules escape from the complex. Therefore, to study the nature of the framework after evacuation of the guest water, guest methanol and coordinated water molecules we have heated **complex 1** at 117 °C for 3 h and subsequently recorded the PXRD data of the heat treated sample. The PXRD analysis indicates that this heat treated sample is crystalline in nature. So, even after the removal of the coordinated and guest water and methanol molecules the host retains its crystallinity. Due to heating, the peak at 9.37° (1st peak) disappears while a new peak appears at 13.56°. Moreover, the intensity of the peak at 10.27° decreases. As the 1st peak appears at a higher angle compared to that of the parent complex (**complex 1**) so it can be inferred that upon thermal treatment shrinking occurs i.e., the supramolecular sheets come closer to each other after heating. The PXRD pattern of this new complex matches well with the simulated XRD pattern of $[Pr(phen)_2Cl_3,H_2O]$ (Fig. 7) [61]. It may therefore be inferred that the structure of the sample obtained by heating **complex 1** at 117 °C is similar to that of $[Pr(phen)_2Cl_3,OH_2]$. Thus, upon removal of guest molecules and coordinated water molecules (partly) by heating, the supramolecular complex undergoes structural changes that leads to the formation of a new complex having the crystal structure similar to that of $[Pr(phen)_2Cl_3,H_2O]$.

The crystalline nature of the partially evacuated complex inspired us to study the flexibility of the complex upon heat treatment. So, this partially evacuated complex was kept in open air. After 14 days, a light green crystalline solid (**complex 1a**) was collected and PXRD pattern of **complex 1a** was recorded. The PXRD pattern shows that the peak at 9.37° reappears which indicates that the heated complex absorb water from air and water molecules enter between the 2D supramolecular metal–organic sheets and this in turn has expanded the channels between the sheets. There are some notable dissimilarity between the PXRD patterns of **complex 1**, **complex 1a** and the partially dehydrated complex. For **complex 1a** the intensity of the peak at 10.27° has diminished and highest peak has been found at 11.27°. Thus it can be concluded that due to soaking of water a new phase has been generated. All the PXRD patterns are presented in the Fig. 7. The results of PXRD study on **complex 1**, **complex 1a** and the partially dehydrated complex have clearly revealed that the MOSH under investigation exhibits *"shrinking and expanding ability"* upon evacuation and reintroduction of guest molecules.

We have examined the thermal behavior of **complex 1a** (Fig. 8). According to Figs. 6 and 8 thermal behavior of **complex 1** and **1a** is different up to 250 °C but it is nearly similar above 250 °C. This difference is due to the fact that **complex 1** contains methanol and water as guest along with the coordinated water molecules while **complex 1a** does not have any methanol molecule. The similarity of thermogravimetric curves of **complex 1** and **1a** indicates that the main structural pattern of the MOSH remains more or less same upon evacuation and reintroduction of guest molecules.

3.5. Temperature and heating time dependent PXRD studies

In order to investigate the mechanism of structural transformation, we have heated **complex 1** at different temperatures and for different time duration at a fixed temperature and we have

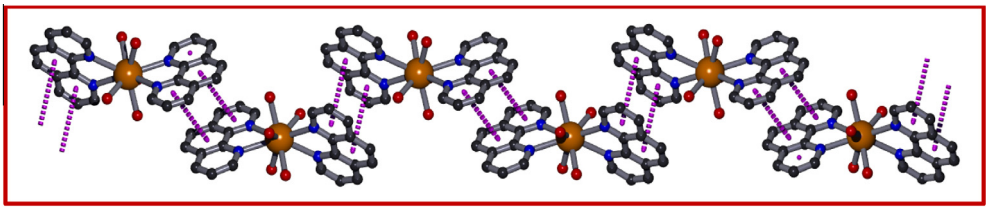

Fig. 2. 1D supramolecular chain is formed along crystallographic *c*-axis by $\pi\cdots\pi$ interactions (Pr = Orange, C = Grey, N = Blue, O = Red). (For interpretation of the references to colour in this figure legend, the reader is referred to the web version of this article.)

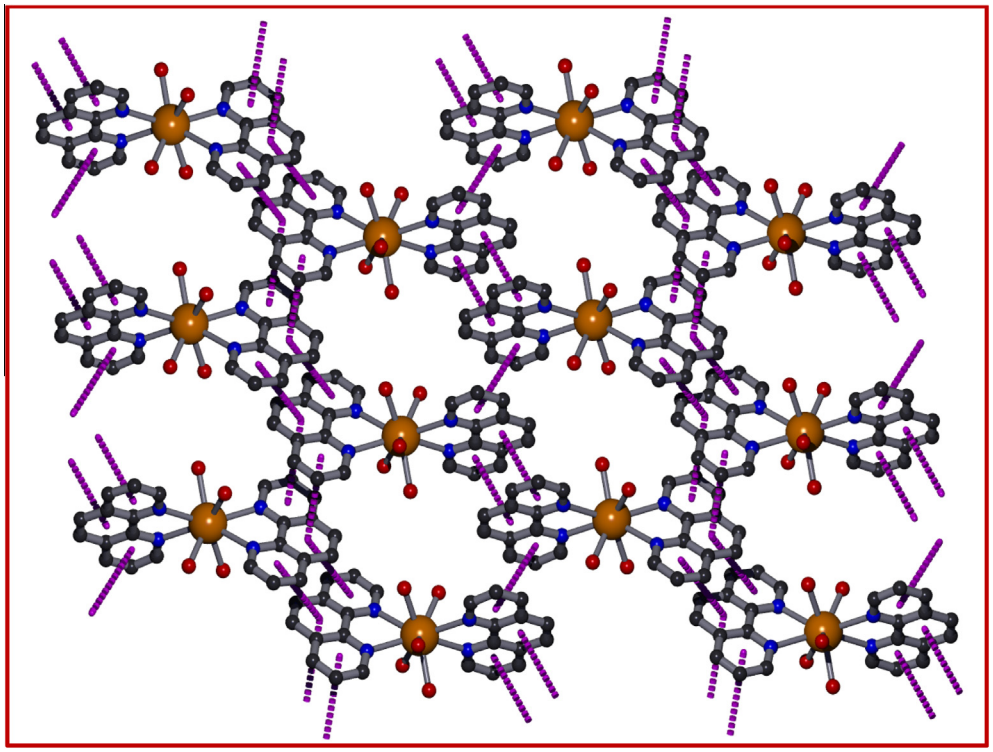

Fig. 3. 1D chains are further connected by π···π interactions to form 2D supramolecular sheets within *ac*-plane (Pr = Orange, C = Grey, N = Blue, O = Red). (For interpretation of the references to colour in this figure legend, the reader is referred to the web version of this article.)

Table 4
π··· interactions of **complex 1**.

$Cg_i\cdots Cg_j$	Cgi···Cgj distance/Å	α/(°)	Cgi perpendicular distance to Cgj	Symmetry
Cg1···Cg5	3.715(2)	1.07(13)	3.4051(11)	2 − *x*, −*y*, 1 − *z*
Cg2···Cg2	4.136(2)	0	3.5163(11)	1 − *x*, −*y*, 1 − *z*
Cg2···Cg5	3.919(2)	1.95(13)	3.5368(11)	1 − *x*, −*y*, 1 − *z*
Cg4···Cg4	3.703(2)	0	3.5580(11)	2 − *x*, −*y*, −*z*
Cg4···Cg6	3.883(2)	3.68(14)	3.5809(12)	2 − *x*, −*y*, −*z*
Cg5···Cg1	3.715(2)	1.07(13)	3.3901(11)	2 − *x*, −*y*, 1 − *z*
Cg5···Cg2	3.919(2)	1.95(13)	3.4800(11)	1 − *x*, −*y*, 1 − *z*
Cg5···Cg5	3.918(2)	0	3.3807(11)	2 − *x*, −*y*, 1 − *z*
Cg6···Cg4	3.883(2)	3.68(14)	3.4788(12)	2 − *x*, −*y*, −*z*
Cg6···Cg6	3.850(2)	0	3.4849(13)	1 − *x*, −*y*, −*z*

Cg1: N1–> C1–> C2–> C3–> C4–> C5–>; Cg2: N2–> C9–> C8–> C10–> C11–> C12–>; Cg4: N4–> C21–> C20–> C22–> C23––> C24–>; Cg5: C4–> C5–> C9–> C8–> C7–> C6–>; Cg6: C16–> C17–> C21–> C20–> C19–> C18–>.

recorded PXRD patterns of the samples obtained after heating (Figs. 9 and 10). We have heated the sample at 75, 100 and 120 °C for 1 h in each case and recorded the PXRD pattern of these heated products. The changes occurred in the PXRD patterns are shown in Fig. 9. The PXRD analysis reveals that upon heating at 75 °C the 1st peak shifts toward higher angle (at 9.67° from 9.43°) and a new sharp peak appears at 13.50° along with the changes in other peaks. The PXRD pattern obtained after heating **complex 1** at 120 °C is distinctly different from all previous phases. We have recorded the PXRD pattern of the sample after heating it at 120 °C for 40 min, 80 min and 120 min. No significant change has been observed in these PXRD patterns (Fig. 10). It may therefore be concluded that with the increase in heating temperature the structural transformation proceeds in stepwise manner through gradual removal of guest molecules. Moreover, upon heating at 120 °C for a certain time the guest water molecule, methanol molecule and three coordinated water molecules get released from the host framework and so a new phase has been produced and no further change occurs.

3.6. Photoluminescence study

For praseodymium (III), there are three possible emitting f-states, e.g., $^3P_0$, $^1D_2$ and $^1G_4$. However, in solution transitions takes place from two excited states ($^3P_0$ and $^1D_2$) [62], and from three excited states ($^3P_0$, $^1D_2$ and $^1G_4$) in solids [63–65]. Moreover, Pr^{3+} also emits efficient ultraviolet 5d-4f-luminescence [80–83] and this transition is used for the fluorometric determination of Pr^{3+} in solutions [65–67].

The emission spectrum of **complex 1** in solid state has been presented in Fig. 11. It is composed of four emission manifolds: the intense $^3P_0 \rightarrow {}^3H_4$ transition at 484 nm, the weak $^3P_0 \rightarrow {}^3H_5$ transition at around 505 nm, a complex band system in 558–670 nm range including the $^1D_2 \rightarrow {}^3H_4$ transition (572 nm), $^3P_0 \rightarrow {}^3H_6$ (592 nm) and $^3P_0 \rightarrow {}^3F_2$ (672 nm) transitions, and the weak $^3P_0 \rightarrow {}^3F_{3,4}$ emission at around 719 nm. The π-π* transition of 1,10-phen appears in the wavelength region of 340–420 nm with a broad band around 384 nm, which can be attributed to the phosphorescence of 1,10-phen [68]. The appearance of such phospho-

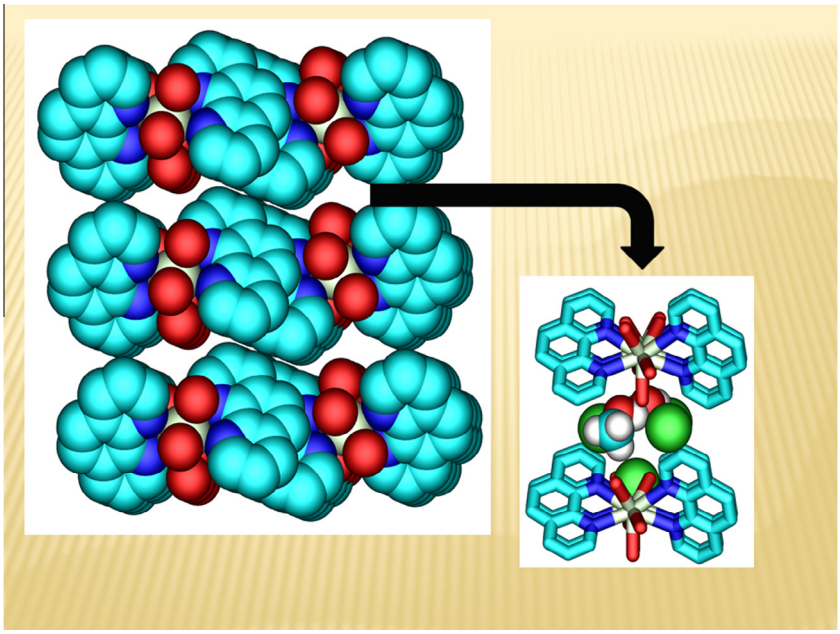

Fig. 4. Supramolecular hosts are filled up by guest molecules (Pr = Grey, C = Cyan, N = Blue, O = Red, Cl = Green). (For interpretation of the references to colour in this figure legend, the reader is referred to the web version of this article.)

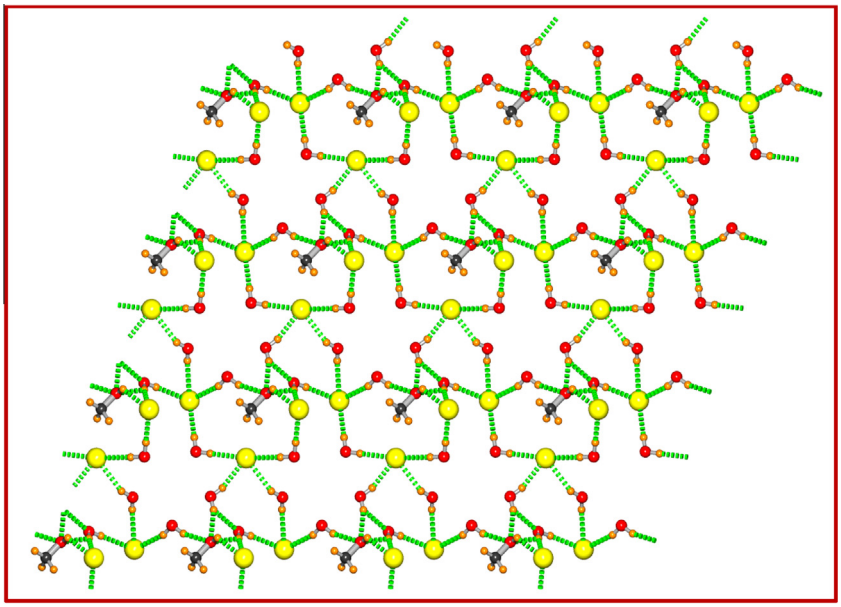

Fig. 5. 2D supramolecular sheet in crystallographic *ab*-plane formed by hydrogen bonding (green) interactions (C = Cyan, O = Red, H =White, Cl = Yellow). (For interpretation of the references to colour in this figure legend, the reader is referred to the web version of this article.)

rescence band at room temperature is a very rare case and it indicates the presence of stable triplet state in 1,10-phen.

The emission spectrum of **complex 1a** (Fig. 12) is nearly similar to that of **complex 1**. It shows an intense $^3P_0 \rightarrow {}^3H_4$ transition at 486 nm, a very weak peak at 500 nm for $^3P_0 \rightarrow {}^3H_5$ transition. A set of peaks with small intensity are also observed within the wavelengths range of 567–670 nm that includes the $^1D_2 \rightarrow {}^3H_4$ (567 nm), $^3P_0 \rightarrow {}^3H_6$ (594 nm) and $^3P_0 \rightarrow {}^3F_2$ (668 nm) transitions. The π-π^* transition of 1,10-phen appears in the wavelength region of 330–415 nm with a broad band around 385 nm, which can be assigned to the phosphorescence of 1,10-phenanthroline. Thus, the photoluminescence property of **complex 1** and **1a** is similar in nature.

3.7. Theoretical study

We performed an *ab initio* geometrical optimization of the H-atom positions at the MP2 level of DFT theory with the 6-31**G(d,p) basis set by freezing the positions of the heavy oxygen atoms for a quantitative understanding of the stability of the water-chloride-methanol cluster. All calculations have been implemented with the GAUSSIAN-03 package [69]. We have performed the calculation with one motif made of six water-one methanol-three chloride, $[(H_2O)_6\text{-}(CH_3OH)\text{-}Cl_3]_n^{3-}$ (**Figure S5**) as it is the basic repeating unit of the whole water-chloride-methanolic sheet. We consider the stabilization energy of the cluster association having n number of water molecules ($E_{n\text{-mer}}$) to be equal to

Table 5
Hydrogen bond dimensions of **complex 1**.

D–H···A	D–H/Å	H···A/Å	D···A/Å	<D–H···A/(°)	Symmetry
O1W–H1W1···Cl2	0.87	2.27	3.110(3)	163	$x, -1+y, z$
O1W–H2W1···O1	0.88	1.91	2.758(5)	163	$1+x, -1+y, z$
O2W–H1W2···O1	0.85	1.95	2.769(5)	162	$1+x, -1+y, z$
O2W–H1W2···O6W	0.85	2.17	2.711(4)	121	$1+x, -1+y, z$
O2W–H2W2···Cl1	0.86	2.24	3.077(2)	164	$1+x, y, z$
O3W–H1W3···Cl1	0.88	2.21	3.092(2)	180	$1+x, y, z$
O3W–H2W3···Cl2	0.87	2.25	3.122(2)	179	
O4W–H1W4···Cl1	0.89	2.21	3.098(2)	179	
O4W–H2W4···Cl3	0.88	2.07	2.949(2)	179	
O5W–H1W5···Cl1	0.82	2.43	3.156(3)	149	
O5W–H2W5···Cl2	0.82	2.46	3.276(2)	169	$x, -1+y, z$
O1–H1O1···Cl3	0.86	1.98	2.444(5)	113	
O6W–H1W6···Cl3	0.87	2.22	3.087(3)	172	
O6W–H1W6···O1	0.87	1.84	2.336(6)	114	
O6W–H2W6···Cl2	0.86	2.32	3.176(4)	173	
C1–H1···O3W	0.95	2.44	3.130(3)	129	
C11–H11···Cl3	0.95	2.74	3.524(3)	140	$x, -1+y, z$
C13–H13···O4W	0.95	2.50	3.087(3)	120	
C19–H19···Cl1	0.95	2.80	3.744(3)	176	$1-x, -y, -z$
C24–H24···O1W	0.95	2.56	2.955(3)	106	
C25–H25B···Cl3	1.00	2.48	2.934(6)	107	
C25–H25C···Cl1	0.96	2.42	3.237(4)	143	

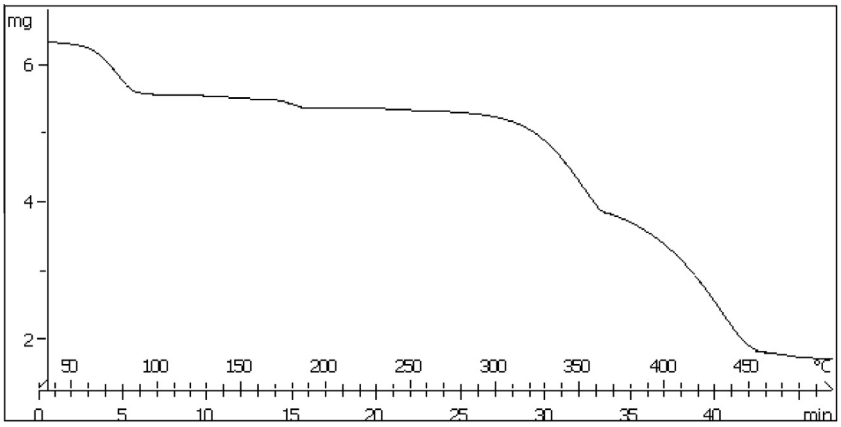

Fig. 6. The thermal plot of **complex 1**.

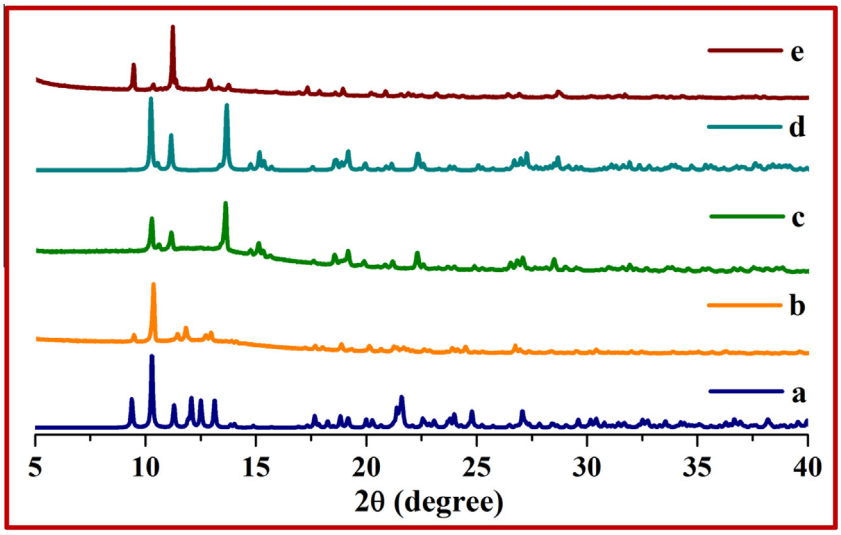

Fig. 7. PXRD patterns of the complexes: (a) simulated pattern of complex; (b) PXRD pattern of the as synthesized material; (c) PXRD pattern of the specimen obtained after removal of guest molecules; (d) simulated pattern of compound reported by M. Khorasani-Motlagh et.al.; (e) PXRD pattern of the compound after re-absorption of water.

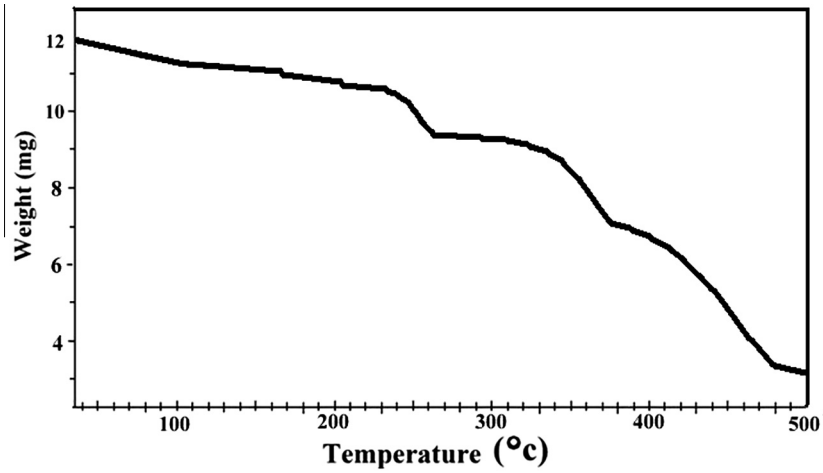

Fig. 8. Thermal plot of **complex 1a**.

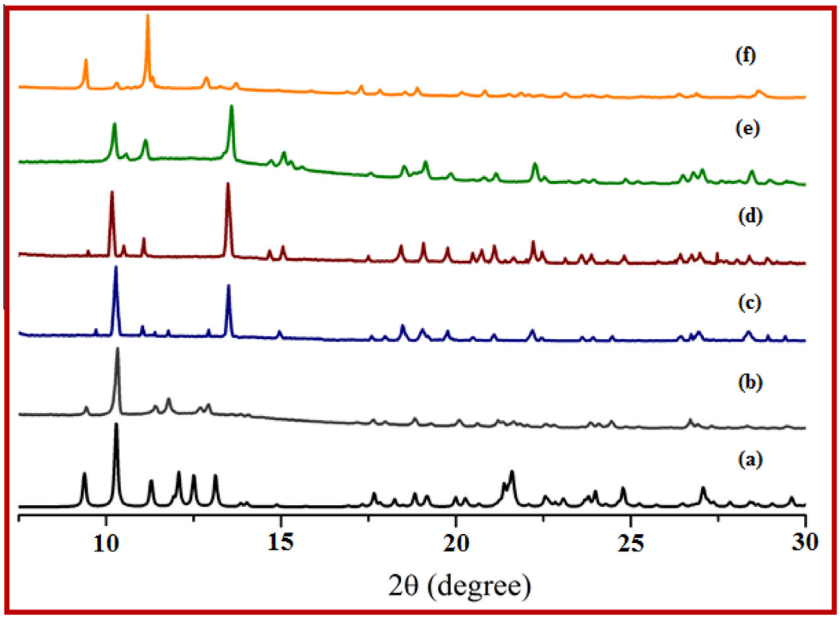

Fig. 9. PXRD patterns (a) black: simulated pattern, (b) deep gray: as synthesized pattern, (c) royal: after heating at 75 °C, (d) wine: after heating at 100 °C, (e) orchid: after heating at 120 °C, (f) orange: after rehydration. (For interpretation of the references to colour in this figure legend, the reader is referred to the web version of this article.)

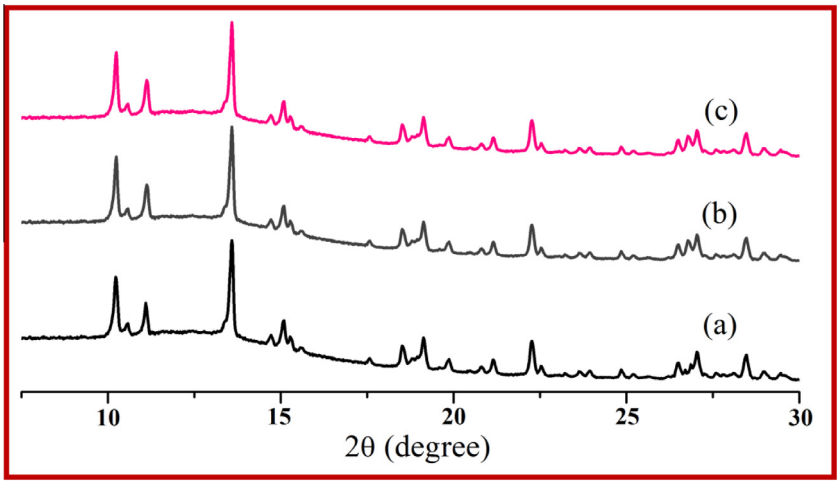

Fig. 10. PXRD patterns (a) black: after heating for 40 min, (b) deep gray: after heating for 80 min, (c) pink: after heating for 120 min at 120 °C. (For interpretation of the references to colour in this figure legend, the reader is referred to the web version of this article.)

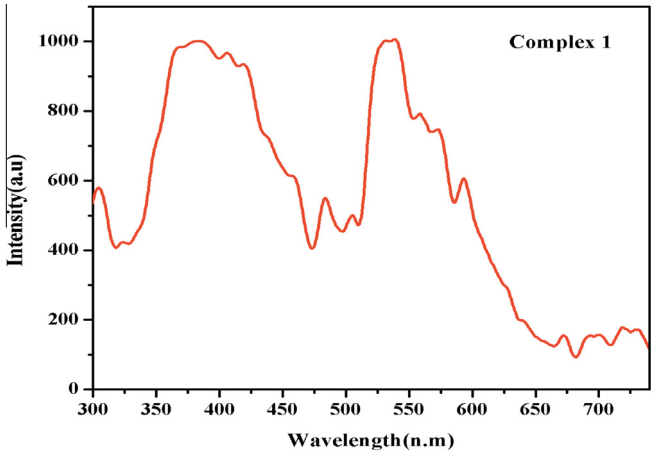

Fig. 11. Photoluminescence spectra of **complex 1**.

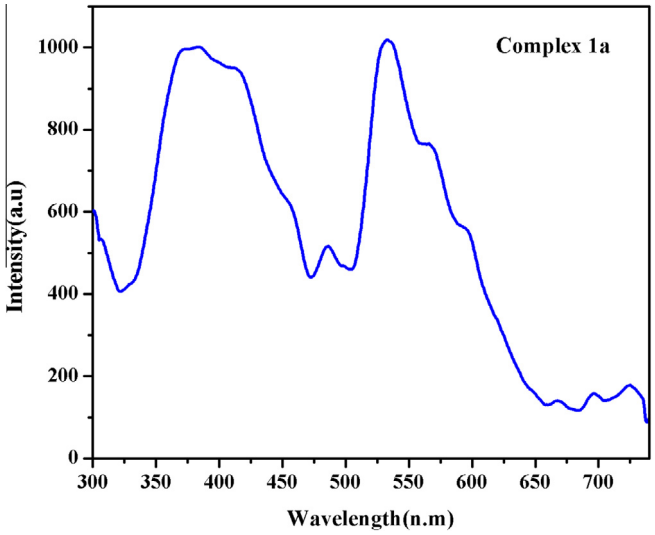

Fig. 12. Photoluminescence spectra of **complex 1a**.

$E_{n\text{-mer}} - (nE_{\text{monomer}})$ and similar approach has been adopted for chloride ion and methanol molecule. The monomeric energy was calculated by optimizing a single H_2O molecule, methanol molecule and chloride ion at the same level of the theory. The basis set superposition error (BSSE) was taken into account following the counterpoise method in the calculation of stabilization energy. The corrected stabilization energy of the $[(H_2O)_6\text{-}(CH_3OH)\text{-}Cl_3]_n^{3-}$ was found to be -1949.427 Kcal mol^{-1} for **complex 1**. The MP2 optimized coordinates of *water-chloride-methanol* cluster for **complex 1** is given in Table S1.

4. Conclusion

In this work, we have shown that hybrid water chloride system can be incorporated in a Pr(III)-based complex synthesized by using a neutral ligand 1,10-phenanthroline. The cationic complex $[Pr(phen)_2(H_2O)_5]^{3+}$ has been stabilized by the counter chloride anions. The 2D sheets are formed within the *ac*-plane by using the $\pi\cdots\pi$ interactions between 1D supramolecular chains formed by connecting the monomeric units. These 2D sheets are further packed by $\pi\cdots\pi$ interactions to form the MOSH having hydrophobic pockets in which guest water, chloride and methanol are stabilized through weak interactions. The hydrogen bonding interactions among coordinated water along with the guests form a unique 2D supramolecular water-chloride-methanol sheet. The guest responsive hydrophobic pockets between 2D supramolecular sheets are flexible in nature. The MOSH can shrink and readjust itself with the retention of crystallinity upon the expulsion and introduction of guest species. It also regains its original shape upon reabsorption of guest species. The present system thus behaves like a dynamic supramolecular metal–organic host which can breathe upon heating and cooling with simultaneous aquation. This dynamic nature is due to the strong affinity of the host towards the guest molecules. The coordination tendency of the Pr(III) ion and the self-assembling tendency of water-chloride and methanol stabilize the system and these are responsible for the affinity of the host towards the guest molecules. The unique hydrogen bonded network of water-chloride and methanol molecules obtained in the present crystalline host will enhance our knowledge on the water-anion assembly and further work may help to understand how water-chloride and methanol may behave in biological processes like chloride ion transportation. In summary, the present crystal structure is a very interesting example of dynamic supramolecular metal–organic host and will act as a guide in the design of further metal–organic host system – where metal coordination tendency towards water molecules and anion-water self-assembling tendency can be utilized.

Acknowledgments

We express our sincere gratitude to Late Dr. Golam Mostafa (1962-2011) for his encouragements and support. We acknowledges financial support from the Council of Scientific and Industrial Research (CSIR), Government of India (through grant number 09/096(0565)2008-EMR-I (for R. S.) and 60(1006)/13-EMR-II). We gratefully acknowledge Prof. R.N. Joardar, Professor (Retd.), Department of Physics, Jadavpur University for helpful discussion. We are grateful to Prof. A. Ghosh, Dept. of Chemistry, University of Calcutta for his kind assistance.

Appendix A. Supplementary material

CCDC contains the supplementary crystallographic data for 821326. These data can be obtained free of charge from The Cambridge Crystallographic Data Centre via www.ccdc.cam.ac.uk/data_request/cif. Supplementary data associated with this article can be found, in the online version, at http://dx.doi.org/10.1016/j.ica.2014.07.077.

References

[1] J.-M. Lehn, Supramolecular Chemistry, VCH, Weinheim, 1995.
[2] J.-M. Lehn, Angew. Chem., Int. Ed. Engl. 29 (1990) 1304.
[3] J.W. Ko, K.S. Min, M.P. Suh, Inorg. Chem. 41 (2002) 2151.
[4] T.K. Maji, P.S. Mukherjee, G. Mostafa, E. Zangrando, N. Ray Chaudhuri, Chem. Commun. (2001) 1368.
[5] L. Carlucci, G. Ciani, M. Moret, D.M. Proserpio, S. Rizzato, Angew. Chem., Int. Ed. 39 (2000) 1506.
[6] S. Biswas, G. Mostafa, I.M. Steele, S. Sarkar, K. Dey, Polyhedron 28 (2009) 1010.
[7] S. Kitagawa, R. Kitaura, S. Noro, Angew. Chem., Int. Ed. 43 (2004) 2334.
[8] G. Ferey, C. Mellot-Draznieks, C. Serre, F. Millange, J. Dutour, S. Surble, I. Margiolaki, Science 309 (2005) 2040.
[9] M. Dincă, J.R. Long, J. Am. Chem. Soc. 129 (2007) 11172.
[10] C.-D. Wu, A. Hu, L. Zhang, W. Lin, J. Am. Chem. Soc. 127 (2005) 8940.
[11] S. Horike, M. Dinc, K. Tamaki, J.R. Long, J. Am. Chem. Soc. 130 (2008) 5854.
[12] S. Hasegawa, S. Horike, R. Matsuda, S. Furukawa, K. Mochizuki, Y. Kinoshita, S. Kitagawa, J. Am. Chem. Soc. 129 (2007) 2607.
[13] H.-Q. Hao, W.-T. Liu, W. Tan, Z. Lin, M.-L. Tong, Cryst. Growth Des. 9 (1) (2009) 1459.
[14] K. Nagayoshi, M.K. Kabir, H. Tobita, K. Honda, M. Kawahara, M. Katada, K. Adachi, H. Nishikawa, I. Ikemoto, H. Kumagai, Y. Hosokoshi, K. Inoue, S. Kitagawa, S. Kawata, J. Am. Chem. Soc. 125 (2003) 221.
[15] M. Ding, J. Wu, Y. Liu, K. Lu, Inorg. Chem. 48 (2009) 7457.
[16] A.L. Gillon, N. Feeder, R.J. Davey, R. Storey, Cryst. Growth Des. 3 (2003) 663.

[17] C. Janiak, T.G. Scharmann, J. Am. Chem. Soc. 124 (2002) 14010.
[18] S. Pal, N.B. Sankaran, A. Samanta, Angew. Chem., Int. Ed. 42 (2003) 1741.
[19] M.T. Ng, T.C. Deivaraj, W.T. Klooster, G.J. McIntyre, J.J. Vittal, Chem. Euro. J 10 (2004) 5853.
[20] A.K. Ghosh, D. Ghoshal, J. Ribas, G. Mostafa, N.R. Chowdhury, Cryst. Growth Des. 6 (2006) 36.
[21] R.R. Fernandes, A.M. Kirillov, C.M. Fatima, G. da Silva, Z. Ma, J.A.L. da Silva, J.J.R.F. da Silva, A.J.L. Pombeiro, Cryst. Growth Des. 8 (2008) 782.
[22] P.S. Lakshminarayanan, E. Suresh, P. Ghosh, Angew. Chem., Int. Ed. 45 (23) (2006) 3807.
[23] R. Custelcean, M.G. Gorbunova, J. Am. Chem. Soc. 127 (2005) 16362.
[24] M.C. Das, S.K. Ghosh, S. Sen, P.K. Bharadwaj, CrystEngComm 12 (2010) 2967.
[25] M.C. Koch, K. Steinmeyer, C. Lorenz, K. Ricker, F. Wolf, M. Otto, B. Zoll, F. Lehmann-Horn, K.H. Grzeschik, T.J. Jentsch, Science 257 (1992) 797.
[26] K. Wichmann, B. Antonioli, T. Söhnel, M. Wenzel, K. Gloe, K. Gloe, J.R. Price, L.F. Lindoy, A.J. Blake, M. Schröder, Coord. Chem. Rev. 250 (2006) 2987.
[27] S. Chakrabarti, M.F.L. Parker, C.W. Morgan, C.E. Schafmeister, D.H. Waldeck, J. Am. Chem. Soc. 131 (2009) 2044.
[28] J.L. Sessler, P.A. Gale, W.-S. Cho, Anion Receptor Chemistry, The Royal Society of Chemistry, 2006.
[29] E.C. Constable, G. Zhang, C.E. Housecroft, M. Neuburger, S. Schaffner, CrystEngComm 11 (2009) 1014.
[30] P.D. Beer, A.P. Gale, Angew. Chem., Int. Ed. 40 (2001) 486.
[31] E.A. Meyer, R.K. Castellano, F. Diederich, Angew. Chem., Int. Ed. 42 (2003) 1210.
[32] L. Infantes, J. Chisholm, S. Motherwell, CrystEngComm 5 (2003) 480.
[33] I. Ravikumar, P.S. Lakshminarayanan, E. Suresh, P. Ghosh, Cryst. Growth Des. 6 (2006) 2630.
[34] P. Ren, B. Ding, W. Shi, Y. Wang, T.B. Lu, P. Cheng, Inorg. Chim. Acta. 359 (2006) 3824.
[35] Z.G. Li, J.W. Xu, H.Q. Via, N.H. Hu, Inorg. Chem. Commun. 9 (2006) 969.
[36] P.S. Lakshminarayanan, D.K. Kumar, P. Ghosh, Inorg. Chem. 44 (2005) 7540.
[37] J. M. Berg, J. L. Tymoczko, L. Stryer, Biochemistry, fifth ed.
[38] R. Saha, S. Biswas, G. Mostafa, CrystEngComm 13 (2011) 1018.
[39] R. Saha, S. Biswas, I.M. Steele, K. Dey, G. Mostafa, Dalton Trans. 40 (2011) 3166.
[40] G.M. Sheldrick, SHELXS 97, Program for Structure Solution, University of Göttingen, Germany, 1997.
[41] G.M. Sheldrick, SHELXL 97, Program for Crystal Structure Refinement, University of Göttingen, Germany, 1997.
[42] A.L. Spek, J. Appl. Crystallogr. 36 (2003) 7.
[43] L.J. Farrugia, J. Appl. Crystallogr. 30 (1997) 565.
[44] L.J. Farrugia, J. Appl. Crystallogr. 32 (1999) 837.
[45] Y.-H. Wana, L.-P. Zhanga, L.-P. Jina, J. Mol. Struct. 658 (2003) 253.
[46] L. Huang, L.-P. Zhang, J. Mol. Struct. 692 (2004) 249.
[47] L. Huanga, L.-P. Zhanga, L.-P. Jin, J. Mol. Struct. 692 (2004) 169.
[48] M. Khorasani-Motlagh, M. Noroozifar, S. Niromand, S. Khajeh, B.O. Patrick, Inorg. Chim. Acta. 362 (2009) 3785.
[49] Y. Li, F.-P. Liang, C.-F. Jiang, X.-L. Li, Z.-L. Chen, Inorg. Chim. Acta. 361 (2008) 219.
[50] O.M. Yaghi, M. O'Keeffe, N.W. Ockwig, H.K. Chae, M. Eddaoudi, J. Kim, Nature 423 (2003) 705.
[51] M.J. Rosseinsky, Microporous Mesoporous Mater. 73 (2004) 15.
[52] S. Kitagawa, R. Kitaura, S.I. Noro, Angew. Chem., Int. Ed. 43 (2004) 2334.
[53] S. Kitagawa, R. Kitaura, S.I. Noro, Angew. Chem. 116 (2004) 2388.
[54] S. Kitagawa, R. Matsuda, Coord. Chem. Rev. 251 (2007) 2490.
[55] G.S. Papaefstathiou, L.R. MacGillivray, Coord. Chem. Rev. 246 (2003) 169.
[56] D.N. Dybtsev, H. Chun, K. Kim, Angew. Chem. 116 (2004) 5143.
[57] R.J. Robson, Chem. Soc. Dalton Trans. (2000) 3735.
[58] B. Moulton, M.J. Zaworotko, Chem. Rev. 101 (2001) 1629.
[59] C.N.R. Rao, S. Natarajan, R. Vaidhyanaathan, Angew. Chem. 116 (2004) 1490.
[60] M. Dincă, A.F. Yu, J.R. Long, J. Am. Chem. Soc. 128 (2006) 8904.
[61] M. Khorasani-Motlagh, M. Noroozifar, S. Niromand, S. Khajeh, B.O. Patrick, Inorganica Chimica Acta. 362 (2009) 3785.
[62] E.B. Sveshnikova, N.T. Timofeev, Opt. Spektroskopiya. 48 (1980) 503.
[63] H. Dornauf, J. Heber, J. Lumin. 20 (1979) 271.
[64] V.P. Dotsenko, N.P. Efryushina, I.V. Berezovskaya, Opt. Spektrosk. 79 (1995) 105.
[65] W. Strek, J. Legendziewicz, E. Lukowiak, K. Maruszewski, J. Sokolnicki, A.A. Boiko, M. Borzechowska, Spectrochim. Acta A. 54 (1998) 2215.
[66] A.G. Svetashev, M.P. Tsvirko, Zh. Prikl, Spektrosk. 62 (1995) 249.
[67] V.T. Mishchenko, D.V. Demeshko, V.A. Perfilev, J. Anal. Chem. 48 (1993) 1268.
[68] M. Hasegawa, A. Ishii, S. Kishi, J. Photochem. Photobiol. A. 178 (2006) 220.
[69] M. J. Frisch, G. W. Trucks, H. B. Schlegel, G. E. Scuseria, M. A. Robb, J. R. Cheeseman, J. A. Jr. Montgomery, T. Vreven, K. N. Kudin, J. C. Burant, J. M. Millam, S. S. Iyengar, J. Tomasi, V. Barone, B. Mennucci, M. Cossi, G. Scalmani, N. Rega, G. A. Petersson, H. Nakatsuji, M. Hada, M. Ehara, K. Toyota, R. Fukuda, J. Hasegawa, M. Ishida, T. Nakajima, Y. Honda, O. Kitao, H. Nakai, M. Klene, X. Li, J. E. Knox, H. P. Hratchian, J. B. Cross, C. Adamo, J. Jaramillo, R. Gomperts, R. E. Stratmann, O. Yazyev, A. J. Austin, R. Cammi, C. Pomelli, J. W. Ochterski, P. Y. Ayala, K. Morokuma, G. A. Voth, P. Salvador, J. J. Dannenberg, V. G. Zakrzewski, S. Dapprich, A. D. Daniels, M. C. Strain, O. Farkas, D. K. Malick, A. D. Rabuck, K. Raghavachari, J. B. Foresman, J. V. Ortiz, Q. Cui, A. G. Baboul, S. Clifford, J. Cioslowski, B. B. Stefanov, G. Liu, A. Liashenko, P. Piskorz, I. Komaromi, R. L. Martin, D. J. Fox, T. Keith, M. A. Al-Laham, C. Y. Peng, A. Nanayakkara, M. Challacombe, P. M. W. Gill, B. Johnson, W. Chen, M. W. Wong, C. Gonzalez and J. A. Pople, Gaussian 03, Revision C.02, Gaussian Inc, Wallingford, CT, 2004.